Available online at www.sciencedirect.com
ScienceDirect
Journal of Sound and Vibration 311 (2008) 824–842
JOURNAL OF SOUND AND VIBRATION
www.elsevier.com/locate/jsvi

A continuous damped vibration absorber to reduce broad-band wave propagation in beams

D.J. Thompson*

Institute of Sound and Vibration Research, University of Southampton, Highfield, Southampton SO17 1BJ, UK

Received 24 January 2007; received in revised form 11 September 2007; accepted 25 September 2007
Available online 31 October 2007

Abstract

In order to attenuate structural waves in beams, a damped mass–spring absorber system is considered that is attached continuously along the beam length. Compared with other measures, such as impedance changes or tuned neutralisers applied at a single point, it is effective for excitation at any location along the beam. Although it is a tuned system, it can also be designed to be effective over a broad frequency range by the use of a high damping loss factor and multiple tuning frequencies. It has the advantage over constrained layer damping treatments that it can be effective even when the structural wavelength is long. The parameters controlling its behaviour are investigated and simple formulae developed, allowing optimisation of its performance. The effective frequency bandwidth increases as the mass ratio of the absorber and the beam is increased and, for moderate-to-high damping, it also increases as the damping loss factor is increased. The maximum decay rate is independent of mass and damping for light damping, but for higher damping it reduces as loss factor increases and increases as the mass ratio increase. A particular application is the reduction of noise from a railway track, which requires the attenuation of structural waves along the rail to be increased over a frequency band of two or more octaves.

1. Introduction

Structural wave propagation in beam structures can lead to unwanted noise transmission and radiation [1,2]. The particular application providing the motivation for the present work is a railway track [3,4] but many other examples exist, such as piping systems for fluids or gases, or beam-like components which are present in structures such as bridges, cranes and buildings. Such beam systems are often very long and may be characterised in the audio frequency range in terms of propagating waves rather than modal behaviour. Whereas geometrical attenuation plays a significant role in two- and three-dimensional structures, in a one-dimensional structure there is no attenuation with distance apart from the effect of damping or discontinuities. Thus, in lightly damped uniform beams, structural waves may propagate over large distances and noise may be transmitted far from its source, to be radiated as sound by the beam itself or by some receiver structure. To reduce the total noise radiated by a vibrating beam, the spatial attenuation must be increased.

The use of a damped mass–spring tuned 'absorber' system applied continuously on a beam is studied here. The purpose of introducing such a system is to attenuate structural waves over a broad frequency range, and

*Tel.: +44 23 8059 2510; fax: +44 23 8059 3190.
E-mail address: djt@isvr.soton.ac.uk

0022-460X/$ - see front matter © 2007 Elsevier Ltd. All rights reserved.
doi:10.1016/j.jsv.2007.09.038

Nomenclature

A	cross-sectional area of beam
E	Young's modulus
I	second moment of area of beam
k	wavenumber in the beam (real part)
k_0	wavenumber of the unsupported beam at ω_0
k_a	wavenumber of the unsupported beam at ω_a
k_b	bending wavenumber in the unsupported beam
m'_a	mass per unit length of absorber
m'_b	mass per unit length of beam
m'_s	mass per unit length of intermediate mass in two layer support
s	stiffness of foundation per unit length
s_1	stiffness of upper foundation layer per unit length
s_2	stiffness of lower foundation layer per unit length
s_a	stiffness of absorber per unit length
S	surface area of beam
v	vibration velocity of beam
w	bending displacement of beam
x	distance along beam
β	wavenumber in the beam (negative imaginary part)
$\delta\omega$	frequency bandwidth of absorber
Δ	decay rate of wave in beam (dB/m)
ε	increment of frequency
η	damping loss factor of foundation
η_1	damping loss factor of upper foundation layer
η_2	damping loss factor of lower foundation layer
η_a	damping loss factor of absorber
η_b	damping loss factor of beam
$\eta_{b,\mathrm{eq}}$	equivalent damping loss factor of beam due to absorber
κ	ratio of stiffnesses s_1/s_2
μ	ratio of absorber mass to beam mass
ω	angular frequency
ω_0	cut-off frequency of beam on elastic foundation
ω_a	tuning frequency of absorber
ω_b	mid-frequency of absorber stop band
ω_c	upper frequency of absorber stop band
ζ	damping ratio

for arbitrarily located excitation. In a specific application of such a system to a railway track, the radiated noise from the track has been reduced by around 6 dB by sufficiently increasing the attenuation of vibration along the rail in a broad frequency band [5,6]. This is achieved by embedding steel masses in an elastomer with a high damping loss factor and attaching this to the rail continuously along its length or in the form of discrete blocks between each sleeper. Other forms of rail absorber have also been developed [6].

The focus in this paper is on determining the effects of the various parameters controlling the behaviour of a generic continuous vibration absorber attached to a beam and deriving simple formulae for this behaviour. After a discussion of the background to the problem and relevant literature, a simple model of a beam on an elastic foundation is first considered. The decay rates of waves in the beam and the effects of the support are illustrated. Using this as a basis, the analysis is extended to an unsupported beam to which a continuous tuned absorber is attached, the absorber being treated as a frequency-dependent complex support stiffness. Approximate formulae are then derived for the effects of the absorber, illustrating simply the influence of mass and damping. The use of multiple tuning frequencies is also considered in order to widen the bandwidth of the absorber. It is then shown that the damping effect of a vibration absorber system attached to a supported beam can be approximated by adding the separate spatial attenuations from the supported beam and the beam with the absorber system. Finally, a system in which the absorber is contained within the foundation is considered.

2. Background and literature review

2.1. Techniques for reduction of vibration in beams

Various vibration control techniques may be used in order to reduce wave propagation in beams [7]. Impedance changes at discontinuities, for example by added stiffness, mass, resilient connections or section

changes, may be used to introduce reflection and thereby reduce transmitted power [2,7]. In practice, such discontinuities cannot always be used, however. In particular for a railway track, continuous welded rail is used to avoid impact noise due to discontinuities in the rail running surface and it is therefore undesirable to reintroduce discontinuities. Tapered terminations with added damping can also be used to reduce reflections from plate or beam edges, for example [8], but are not applicable to the infinite beam of constant cross-section considered here.

To increase the damping, constrained layer or unconstrained layer damping treatments are particularly effective for relatively thin plate systems [7,9], but beams are often stiffer in order to carry structural loads. Consequently, the structural wavelengths are long and surface strains are small so that, to be effective, the corresponding damping treatments would become impractically large. A tuned absorber system responds to surface motion rather than strain and can therefore be arranged to be efficient at low frequencies [10].

2.2. Vibration absorbers

Mass–spring or mass–spring–damper systems are widely used to control the response of resonant structures [7,9,11,12]. These are variously called tuned vibration absorbers, dynamic vibration absorbers, tuned mass dampers or vibration neutralisers. The design of the system differs depending on whether the purpose is to suppress the response at a troublesome resonance frequency due to a broad-band excitation or to suppress the response at a troublesome forcing frequency. Following Ref. [11] they may be called dynamic *absorbers* in the former case and vibration *neutralisers* in the latter case.

The performance in both situations increases as the added mass is increased. However, the need for damping in the added system depends on the application. When applied to deal with a resonance there is an optimum value of the damping; if it is too high the response is not modified at the original resonance, but if it is too low the response at modified resonances of the coupled system will remain a problem. In practice, relatively high values of damping loss factor are usually required for effective results [11]. On the other hand, to tackle a troublesome forcing frequency, the damping should be low to obtain good performance at the intended frequency. The low damping means that the bandwidth of operation becomes small. Therefore, in order to cover a broader frequency range, for example to allow for variations in the forcing frequency, either the damping has to be compromised or an adaptive system may be used [13]. Note that the term 'absorber' will be used throughout the remainder of this paper, even when discussing undamped cases, as the practical applications envisaged have broad-band excitation and will generally require high damping.

The theory of the dynamic vibration absorber was first presented by Ormondroyd and Den Hartog [14]. Since then, dynamic absorbers have been applied in a wide variety of situations. Many examples of applications and various practical designs are discussed by Hunt [12].

At its resonance frequency an undamped mass–spring system pins the host structure; it should therefore be tuned to the resonance of the original structure. However, to give the best effect over a frequency band under random excitation, Den Hartog [15] derived optimum values for the frequency of a damped absorber and its damping ratio in order to minimise the displacement response of the host structure. The absorber frequency should be tuned to $\omega = \omega_m/(1+\mu)$, where ω_m is the natural frequency of the original resonance to be damped and μ is the ratio of absorber mass to the (modal) mass of the host structure. The optimum damping ratio is found to be $\zeta = (3\mu/(8(1+\mu)^3))^{1/2}$ (a list of symbols is given in Nomenclature).

Vibration absorbers are generally intended to deal with a single resonance of the host structure and they therefore have only a small effect at other structural resonances that lie far from the tuning frequency [7]. It is possible to add multiple absorbers on a structure, tuned to deal with different resonances. For example, Rana and Soong [16] considered applying three absorbers to a three-degree-of-freedom building model to reduce the response to earthquake excitation, but they found that the addition of absorbers intended to deal with the second and third modes led to a slight increase in the response at the first mode due to the additional mass.

A recent high-profile vibration problem was the excessive lateral sway motion caused by crowds walking across the Millennium footbridge in London in June 2000 [17,18]. In an extensive review of this field, dynamic vibration absorbers were identified as a common solution for both lateral and vertical motion of footbridges [19]. Other solutions include viscous dampers and the tuning of natural frequencies to avoid the main frequency region of excitation due to pedestrian-induced forces. The Millennium Bridge was

subsequently modified to increase its damping substantially by a combination of viscous dampers and vibration absorbers [17,19].

2.3. Application to waves in beams

Although most applications of dynamic absorber systems have been to resonant finite systems, lightly damped tuned neutralisers have also been considered for application at a point on a long beam to form an impedance change tuned to a particular forcing frequency [20,21]. Due to the influence of near-field waves in the beam, the maximum blocking effect occurs at a frequency just above the tuning frequency of the mass–spring system if the system is arranged to apply a point force. At the tuning frequency itself only half of the incident energy in a bending wave is reflected, since the neutraliser effectively pins the beam. In Ref. [20] the bandwidth of such a neutraliser, defined there as the frequency range over which the attenuation is greater than 3 dB, is found to be equal to $\omega_a \mu k/4$, where ω_a is the tuning frequency (the natural frequency of the grounded mass–spring system), k is the bending wavenumber in the beam and μ is the ratio of the mass of the neutraliser to the mass per unit length of the beam.

Such a mass–spring system applied at a single point is not suitable for attenuating structural wave propagation in a beam over a wide frequency range. Moreover, if the excitation can, in principle, be at any location along the beam, as is the case for a railway track, it is clear that some form of distributed treatment is required.

2.4. Distributed vibration absorbers

Applications of vibration absorbers distributed across a structure are much less common than those applied at a point intended to deal with particular modes of the structure. Kashina and Tyutekin [22] describe the use of a set of undamped resonators to reduce longitudinal or flexural waves in beams or plates. They envisage a group of mass–spring systems located over a certain length of the beam or plate and derive relations for the optimum mass and number of oscillators required to give a certain attenuation over a specified frequency band.

Smith et al. [23] give an analysis of a beam or plate with a continuous layer of absorbers applied to it. Their interest was in ship hulls. It was recognised that there is potential to use the mass of installed machinery in the ship as a distributed absorber with a high mass ratio. Analysis of an undamped absorber showed that waves in the beam (or plate) have a wavenumber with an imaginary part (i.e. strong decay) in the frequency range $1<\omega/\omega_a<(1+\mu)^{1/2}$ where ω_a is the absorber tuning frequency and μ is the ratio of absorber mass to beam mass [23]. It was recognised that adding damping to an array of dynamic absorbers on a plate or beam will reduce the wave attenuation at its peak value but spread the effect over a wider bandwidth. Numerical results were presented which showed this, but no analysis was given of the bandwidth or attenuation in the damped case. Experiments were presented on an aluminium beam, which confirmed the predictions. It was also demonstrated experimentally that there is additional benefit if the absorber mass is distributed between two different tuning frequencies.

This work does not appear to have led to the development of distributed vibration absorbers for attenuating structural waves. Strasberg and Feit [24] present a derivation of the damping effect of a set of small oscillators attached to a large main structure, representing attached substructures. They show that the damping effect is primarily determined by the attached mass and not the damping of the attached systems. Other papers discussing distributed absorbers are generally concerned with the control of modes of vibration [10] or the control of acoustic transmission, for example in aerospace structures [25–27].

3. Beam on elastic foundation

3.1. Undamped case

Before studying a continuous vibration absorber attached to a beam, it is helpful to review the results for a beam on an elastic foundation. Throughout, for clarity, the analysis is restricted to an Euler–Bernoulli beam,

although it could readily be extended to a Timoshenko beam. Consider a uniform beam with bending stiffness EI and mass per unit length m_b' on an elastic foundation of stiffness per unit length s, as shown in Fig. 1. Initially damping is omitted. Considering harmonic motion at frequency ω, the free vibration satisfies [1]

$$EI\frac{\mathrm{d}^4 w}{\mathrm{d}x^4} + (s - m'_b\omega^2)w = 0, \tag{1}$$

where w is the complex vibration amplitude and x is the coordinate along the beam direction. Seeking free wave solutions of the form $\mathrm{e}^{-\mathrm{i}\tilde{k}x}$, the wavenumber in the supported beam, $\tilde{k} = k - \mathrm{i}\beta$, which may in principle be complex, has solutions

$$\tilde{k}^2 = \pm\sqrt{\frac{m'_b\omega^2 - s}{EI}} = \pm k_b^2\sqrt{1 - \frac{\omega_0^2}{\omega^2}}, \tag{2}$$

where $\omega_0 = (s/m_b')^{1/2}$ is the resonance frequency of the beam mass on the support stiffness and $k_b = (\omega^2 m_b'/EI)^{1/4}$ is the wavenumber of free waves in the unsupported beam. In the absence of damping, the wavenumber $\tilde{k}$ has purely real and imaginary solutions for frequencies above ω_0. These wavenumbers are always smaller in magnitude than the corresponding ones for the unsupported beam, k_b, but tend towards k_b at high frequency. At $\omega = \omega_0$, $\tilde{k} = 0$ and the wavelength of free wave propagation becomes infinite, meaning that the whole beam moves in phase along its length. This is referred to as the cut-off frequency for free waves in the supported beam (or sometimes 'cut-on' frequency).

For frequencies below ω_0, free wave propagation cannot occur. Instead, all waves have a wavenumber $\tilde{k}$ with a non-zero imaginary part β that is equal in magnitude to the real part, and waves occur in complex conjugate pairs. These waves are attenuated rapidly along the beam length. For $\omega \ll \omega_0$, the wavenumber in the fourth quadrant of the complex plane satisfies

$$k = \beta \approx \frac{k_0}{\sqrt{2}}, \tag{3}$$

where $k_0 = (s/EI)^{1/4}$ is the wavenumber of the unsupported beam at frequency ω_0.

The attenuation of a wave along the beam is determined by the imaginary part β and is zero for the propagating waves above ω_0 in the absence of damping. For a complex wavenumber $\tilde{k} = k - \mathrm{i}\beta$, the amplitude reduces over a distance of 1 m by a factor $\exp(-\beta)$. The decay rate Δ may be expressed in dB/m and is given by

$$\Delta = 20\log_{10}(\exp(\beta)) = 8.686\beta. \tag{4}$$

The rate of attenuation of vibration along the beam is important for the noise radiated. The total sound power radiated by a damped propagating wave in an infinite beam is inversely proportional to β and hence to the decay rate, Δ.

3.2. Effect of damping

Introducing damping into the support by means of a complex stiffness, $s \to s(1 + \mathrm{i}\eta)$ and similarly for the beam $EI \to EI(1 + \mathrm{i}\eta_b)$, gives complex wavenumbers

$$\tilde{k} = k_b(1 + \mathrm{i}\eta_b)^{-1/4}\left(1 - \left(\frac{\omega_0}{\omega}\right)^2(1 + \mathrm{i}\eta)\right)^{1/4}. \tag{5}$$

Three particular cases can be considered:

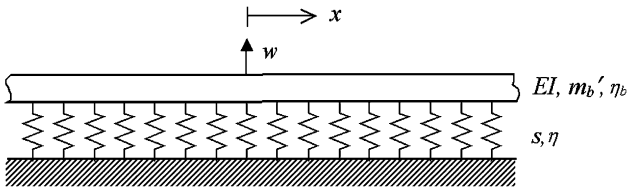

Fig. 1. Beam on elastic foundation.

(i) At high frequency, for $\omega \gg \omega_0$, the real part, $k \approx k_b$. The imaginary part is given by

$$\beta \approx k_b\left(\frac{\eta_b}{4}+\frac{\eta}{4}\left(\frac{\omega_0}{\omega}\right)^2\right). \tag{6}$$

(ii) At the cut-off frequency, $\omega = \omega_0$, support damping dominates and $k \approx (-i\eta s/EI)^{1/4}$. The root with the smallest imaginary part (and hence the lowest attenuation) is $\tilde{k} = e^{-i\pi/8}(\eta s/EI)^{1/4}$. This gives, $k = 0.924\,\eta^{1/4}k_0$, $\beta = 0.383\,\eta^{1/4}k_0$.

(iii) For $\omega \ll \omega_0$, the attenuation is large. The addition of damping has negligible effect and the wavenumber is given approximately by Eq. (3).

Fig. 2 shows the wavenumber and wave decay rate in non-dimensional form for various values of damping loss factor. The frequency is shown relative to the cut-off frequency ω_0 whilst the real and imaginary parts of the wavenumber are non-dimensionalised by dividing by k_0, the wavenumber in the unsupported beam at ω_0.

The real part of the wavenumber is affected by damping only in the vicinity of ω_0, where increasing the support damping η leads to an increase in the magnitude at the minimum. Results for different values of beam damping loss factor, η_b, are indistinguishable and therefore not shown. Both real and imaginary parts of $\tilde{k}/k_0$ tend to $1/\sqrt{2}$ at low frequency, see Eq. (3). At high frequency the real part, k tends to k_b which is proportional to $\omega^{1/2}$. The high-frequency behaviour of β can be seen to follow Eq. (6), with a slope of $\omega^{-3/2}$ in the absence of beam damping or $\omega^{1/2}$ where beam damping dominates. Extrapolating this high-frequency behaviour back to $\omega = \omega_0$ gives $\beta/k_0 \to \eta/4$ or $\eta_b/4$, respectively. It can be seen that adding damping to the beam is effective over a much wider frequency range than adding damping to the support.

For a railway track, ω_0 is typically equivalent to frequencies in the range 200–800 Hz, depending on the rail support stiffness. Above this frequency free wave propagation occurs and significant sound radiation occurs [30]. Decay rates are typically about 10 dB/m at low frequency, falling to around 1 dB/m above the cut-off frequency. The rail damper described in Ref. [5] is designed to increase this decay rate in the frequency region where the rail is the dominant source of noise, which is typically a band of at least two octaves wide above the cut-off frequency.

4. Beam with attached continuous vibration absorber

Next, a beam is considered to which a continuous mass–spring system is attached, as shown in Fig. 3. The beam is considered without any support stiffness in order to separate the effects of the absorber more readily;

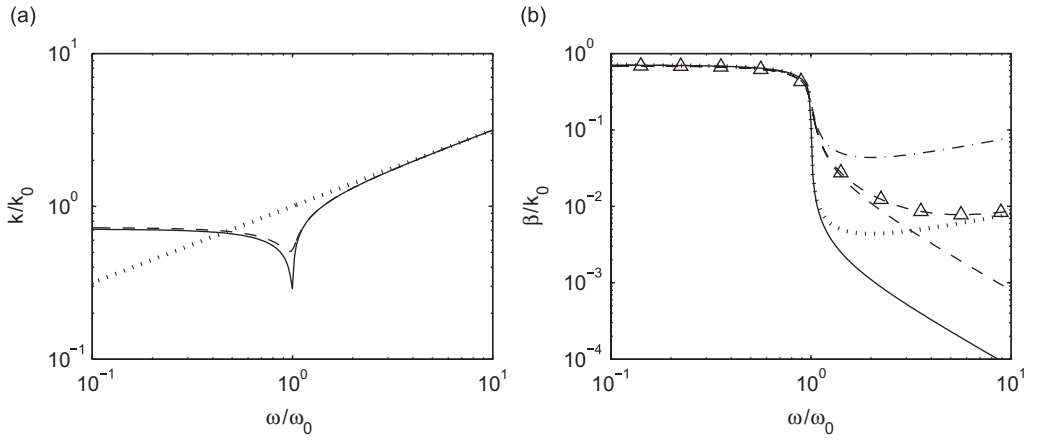

Fig. 2. Wavenumbers of a beam on an elastic foundation: (a) real part for $\eta_b = 0$: —, $\eta = 0.01$; – – –, $\eta = 0.1$, · · · · · ·, unsupported beam; (b) imaginary part: —, $\eta = 0.01$, $\eta_b = 0$; – – –, $\eta = 0.1$, $\eta_b = 0$; · · · · · ·, $\eta = \eta_b = 0.01$; –Δ–, $\eta = 0.1$, $\eta_b = 0.01$; – · –, $\eta = \eta_b = 0.1$.

the combined effect will be considered in Section 7 below. The bending stiffness of the absorber mass is ignored as this will usually be much more flexible than the beam itself.

4.1. Frequency-dependent stiffness

The absorber is assumed to have mass per unit length m_a' and stiffness per unit length s_a. These are related by the 'tuning frequency' of the absorber, $\omega_a = (s_a/m_a')^{1/2}$ which is the resonance frequency of the mass–spring system when attached to a rigid foundation. Hysteretic damping is added to the springs using a loss factor η_a. The analysis of Section 3 can be used directly by replacing s by a frequency-dependent 'support stiffness', $s(\omega)$ describing the attached mass–spring system, which is given by

$$s(\omega) = \frac{\omega^2 s_a(1+\mathrm{i}\eta_a)}{\omega^2 - \omega_a^2(1+\mathrm{i}\eta_a)}. \tag{7}$$

At high frequency, $\omega \gg \omega_a$, $s(\omega)$ can be approximated by the damped absorber stiffness,

$$s(\omega) \to s_a(1+\mathrm{i}\eta_a) \quad \text{for } \omega \gg \omega_a \tag{8}$$

and the beam can be expected to have similar behaviour to that described in Section 3. At ω_a, the denominator of Eq. (7) is zero for an undamped system, giving $s(\omega) \to \infty$. For a damped system this becomes

$$s(\omega) \approx s_a\left(\frac{\mathrm{i}}{\eta_a} - 1\right) \quad \text{for } \omega \approx \omega_a. \tag{9}$$

The imaginary part of $s(\omega)$ is thus large in the vicinity of ω_a. Below ω_a, the real part of $s(\omega)$ is negative (mass-like), and at low frequencies it is determined by the absorber mass, which becomes effectively rigidly connected to the beam. However, $s(\omega)$ also has a small imaginary part in this region which will prove to be important, so that it is useful to retain the second-order terms to give

$$s(\omega) \approx -\omega^2 m'_a\left(1 + \frac{\omega^2}{\omega_a^2(1+\mathrm{i}\eta_a)}\right) \quad \text{for } \omega \ll \omega_a \tag{10}$$

The wavenumber in the beam in the presence of the mass–spring system is found using Eq. (7) as

$$\tilde{k}^4 = k_b^4\left(1 + \mu\frac{1+\mathrm{i}\eta_a}{1+\mathrm{i}\eta_a - (\omega^2/\omega_a^2)}\right), \tag{11}$$

where μ is the ratio of the absorber mass to the beam mass, m_a'/m_b'.

4.2. Undamped absorber

Considering first an undamped vibration absorber, $\eta_a = 0$, below ω_a the wavenumber will be increased by the presence of the absorber, as $s(\omega)$ is mass-like. At low frequencies the effective mass of the beam becomes $m_b' + m_a'$ but as the frequency approaches ω_a the effective mass becomes large and the wavenumber increases towards infinity. Above the tuning frequency, $s(\omega)$ is stiffness-like, initially with a very large stiffness. Therefore a blocked region can be expected, where $\tilde{k}^2$ is imaginary, in the same way as for the beam on elastic foundation below its cut-off frequency.

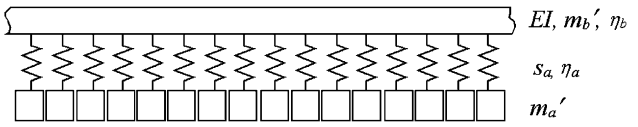

Fig. 3. Beam connected to continuous mass–spring system.

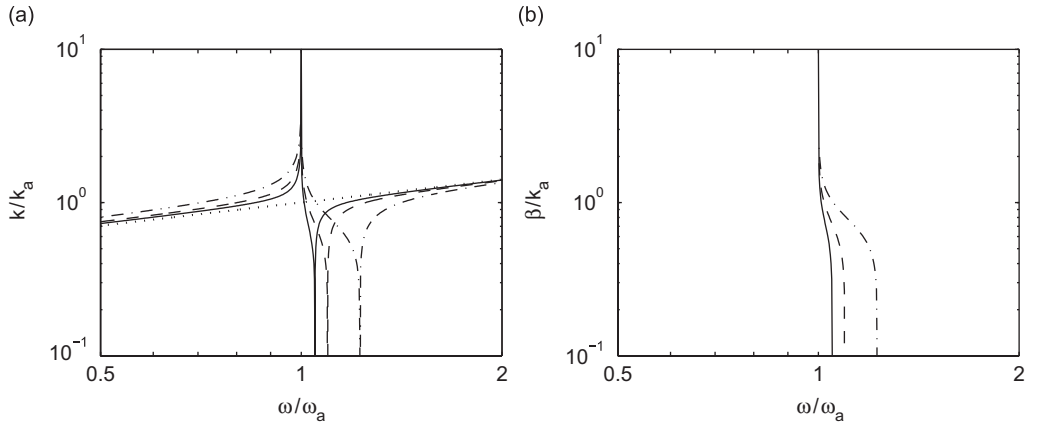

Fig. 4. Wavenumbers of beam with undamped tuned absorber. —, $\mu = 0.1$, – – –, $\mu = 0.2$; – · – · $\mu = 0.5$, · · · · · ·, $\mu = 0$: (a) real part of first wave, (b) imaginary part of first wave.

For the undamped absorber, this blocked region will extend from ω_a to the cut-off frequency of free waves in the beam, ω_c, which is given by setting $\tilde{k} = 0$. This is satisfied by

$$\omega_c = \omega_a\sqrt{1+\mu} \approx \omega_a\left(1+\frac{\mu}{2}\right) \quad \text{for } \mu \ll 1 \tag{12}$$

as found by Smith et al. [23]. The wavenumbers are shown in Fig. 4 for various mass ratios. These have been normalised by the free beam wavenumber at ω_a, denoted $k_a = (\mu s_a/EI)^{1/4}$. In the blocked region, between ω_a and ω_c, the wavenumbers are large and in conjugate pairs. For practical parameters, $\mu \ll 1$ and the undamped absorber has a fairly narrow blocked region.

In the absence of damping, non-zero spatial attenuation only occurs in the blocked region; elsewhere $\tilde{k}$ is real. At ω_a the decay rates tend to infinity, while at ω_c they tend to 0, as seen in Fig. 4(b). Between these extremes the mass ratio affects the width of the blocked region but not the magnitude of the decay rates within this region.

This can also be shown analytically by considering the frequency ω_b given by $\omega_b^2 = \omega_a^2(1+\mu/2)$ at the centre of the blocked region. For the undamped case Eq. (7) gives

$$s(\omega_b) = 2\omega_b^2 m'_b. \tag{13}$$

Hence, the wavenumber at ω_b is given by

$$\tilde{k} = k_b(-1)^{1/4} = k_b\frac{1-\mathrm{i}}{\sqrt{2}}, \tag{14}$$

which is independent of μ for $\mu \ll 1$. It increases slightly if μ is large, as k_b will be slightly higher at ω_b than at ω_a.

4.3. Damped absorber

By adding damping to the mass–spring system, the frequency range in which beam vibration is attenuated can be increased. Results obtained for different damping loss factors are shown in Fig. 5 for an absorber mass of $\mu = 0.2$ and 0.5. The imaginary part of the wavenumber is again shown normalised by the free beam wavenumber at ω_a.

Clearly, as the damping is increased, particularly for large values, the decay rate at the peak is reduced whilst the height of the flanks is increased. Comparing the two figures, it can be seen that, as the mass ratio is increased, the blocked region becomes wider, as was seen in Fig. 4 for the undamped case, while the decay rate at the flanks is increased. In practical applications the mass should be as large as possible within practical constraints. The rail damper described in Ref. [5] had a total mass ratio of about 0.25. The optimal value of damping loss factor depends on the shape of the excitation spectrum and therefore cannot be generalised.

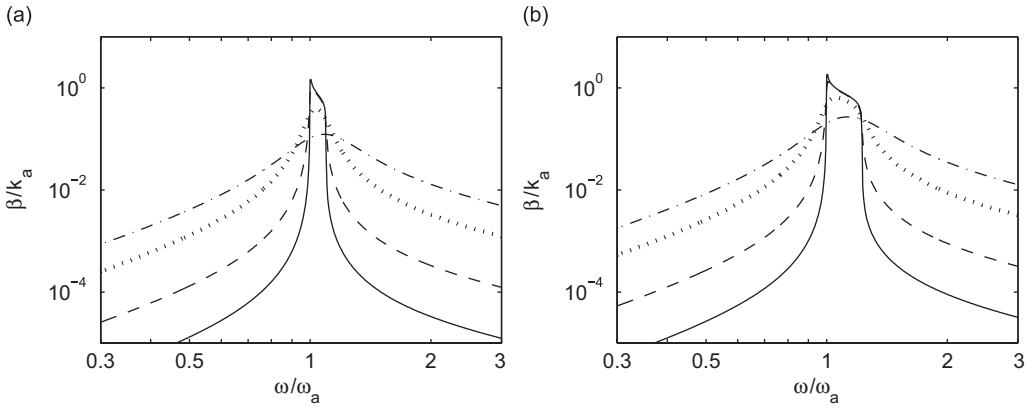

Fig. 5. Normalised decay rate of beam with tuned absorber: (a) $\mu = 0.2$, (b) $\mu = 0.5$. —, $\eta_a = 0.001$; – – –, $\eta_a = 0.01$; · · · · · ·, $\eta_a = 0.1$; – · – · –, $\eta_a = 0.4$.

5. Approximate formulae

5.1. Approximate formulae for the decay rate far from the tuning frequency

The effects shown in Fig. 5 can be demonstrated analytically. First the decay rate far from the tuning frequency is considered. From Eq. (2) the imaginary part of the wavenumber is

$$\beta = -k_b \,\mathrm{Im}\left\{\left(1 - \frac{s(\omega)}{m'_r\omega^2}\right)^{1/4}\right\}. \tag{15}$$

At high frequencies, from Eq. (8) and substituting $s_a = m_a'\omega_a{}^2$,

$$\beta \approx \frac{k_b}{4}\frac{\omega_a^2}{\omega^2}\mu\eta_a \quad \text{for } \omega \gg \omega_a. \tag{16}$$

Similarly at low frequencies, for small values of μ and η_a it is found that

$$\beta \approx \frac{k_b}{4}\frac{\omega^2}{\omega_a^2}\mu\eta_a \quad \text{for } \omega \ll \omega_a. \tag{17}$$

Comparing Eq. (16) and (17), these both increase directly in proportion to the mass ratio μ and the damping loss factor η_a, as seen in Fig. 5.

The frequency dependence is complicated by the presence of k_b which is proportional to $\omega^{1/2}$ so that below the tuning frequency β is proportional to $\omega^{5/2}$ while at high frequency it decreases with $\omega^{-3/2}$. It is possible to simplify the interpretation by considering an equivalent loss factor of the beam, which will be defined by (compare Eq. (6))

$$\eta_{b,\mathrm{eq}} = \frac{4\beta}{k_b}. \tag{18}$$

Thus,

$$\eta_{b,\mathrm{eq}} \approx \frac{\omega^2}{\omega_a^2}\mu\eta_a \quad \text{for } \omega \ll \omega_a, \tag{19}$$

$$\eta_{b,\mathrm{eq}} \approx \frac{\omega_a^2}{\omega^2}\mu\eta_a \quad \text{for } \omega \gg \omega_a. \tag{20}$$

These results only apply at very low levels of decay rate and cannot be used to determine a useful frequency 'bandwidth' of the absorber effect. From Fig. 5 it can be seen that the straight parts of the graphs only occur well below $\omega_a/2$ and above $2\omega_a$. The curved flanks will be considered further in Section 5.3 below.

5.2. Approximate formulae for the decay rate in the blocked zone

In this section the decay rate at the peak will be determined. In order to estimate this, it is convenient to consider the frequency ω_b given in Section 4.2 above, which is at the centre of the blocked zone for the undamped case. Evaluating the imaginary part of the wavenumber at this frequency from Eq. (15),

$$\beta = -k_b \mathrm{Im}\left\{\left(1 - \frac{\mu(1+\mathrm{i}\eta_a)}{\mu/2 - \mathrm{i}\eta_a}\right)^{1/4}\right\} \quad \text{for } \omega = \omega_b. \tag{21}$$

Two extreme cases can be considered. Firstly, for small damping $\eta_a \ll \mu/2$ (and $\eta \ll 1$):

$$\beta \approx -k_b \mathrm{Im}\left\{\left(-1 - 2\mathrm{i}\eta_a - 2\mathrm{i}\frac{\eta_a}{\mu}\right)^{1/4}\right\}. \tag{22}$$

Here the imaginary terms inside the brackets are small compared with -1, so that the decay rate is given by the earlier result for the undamped case, see Eq. (14), which is independent of both the mass ratio and the loss factor. The 'equivalent loss factor' of the beam is $\eta_{b,\mathrm{eq}} \approx 2\sqrt{2} = 2.83$.

Secondly, for large damping $\eta_a \gg \mu/2$ (and $\mu \ll 2$), Eq. (21) reduces to

$$\beta = \frac{k_b}{4}\frac{\mu}{\eta_a} \tag{23}$$

This increases as the mass ratio increases but *reduces* as the damping of the absorber increases. The equivalent loss factor of the beam is

$$\eta_{b,\mathrm{eq}} = \frac{\mu}{\eta_a}. \tag{24}$$

Reference to Fig. 5 confirms that the damping effect in the blocked region is independent of η_a at low values and then reduces as η_a increases according to Eq. (23). Moreover, for high values of η_a, the height in the blocked region is increased as μ increases.

5.3. Bandwidth of absorber

In order to determine the bandwidth of the absorber, that is, the frequency bandwidth for which the decay rate (or equivalent loss factor) is above a certain value, consider frequencies in the vicinity of ω_a and write $\omega = \omega_a(1+\varepsilon)$. Then provided that $|\varepsilon| \ll 1$, from Eq. (11)

$$\frac{\eta_{b,\mathrm{eq}}}{4} = \frac{\beta}{k_b} \approx -\mathrm{Im}\left\{\left(1 + \mu\frac{(1+\mathrm{i}\eta_a)}{\mathrm{i}\eta_a - 2\varepsilon}\right)^{1/4}\right\}. \tag{25}$$

Expanding

$$\frac{\eta_{b,\mathrm{eq}}}{4} \approx -\mathrm{Im}\left\{\left(\frac{1 + \left(2\varepsilon/\eta_a\right)^2 + \mu - (2\varepsilon\mu/\eta_a^2) - (\mathrm{i}\mu/\eta_a)(1+2\varepsilon)}{1 + \left(2\varepsilon/\eta_a\right)^2}\right)^{1/4}\right\}. \tag{26}$$

Provided that $\eta_{b,\mathrm{eq}} \ll 4$, the imaginary part of the expression inside the round brackets will be small compared with the real part, allowing it to be expressed as

$$\begin{aligned}\eta_{b,\mathrm{eq}} &\approx \left(\frac{1 + \left(2\varepsilon/\eta_a\right)^2 + \mu - (2\varepsilon\mu/\eta_a^2)}{1 + \left(2\varepsilon/\eta_a\right)^2}\right)^{1/4}\left(\frac{(\mu/\eta_a)(1+2\varepsilon)}{1 + \left(2\varepsilon/\eta_a\right)^2 + \mu - (2\varepsilon\mu/\eta_a^2)}\right)\\ &= \frac{\mathrm{Re}(\tilde{k})}{k_b}\left(\frac{(\mu/\eta_a)(1+2\varepsilon)}{1 + \left(2\varepsilon/\eta_a\right)^2 + \mu - (2\varepsilon\mu/\eta_a^2)}\right).\end{aligned} \tag{27}$$

For $|\varepsilon| \ll 1$, $\mathrm{Re}(\tilde{k}) \approx k_b \approx k_a$. The remaining expression can be solved for ε:

$$\eta_{b,\mathrm{eq}}\left(1+\left(\frac{2\varepsilon}{\eta_a}\right)^2+\mu-\frac{2\varepsilon\mu}{\eta_a^2}\right)\approx\frac{\mu}{\eta_a}(1+2\varepsilon). \tag{28}$$

This has two roots ε_+ and ε_- which are above and below zero (either side of ω_a) so that the bandwidth $\delta\omega$ within which $\eta_{b,\mathrm{eq}}$ is greater than a certain value is given by

$$\frac{\delta\omega}{\omega_a}=\varepsilon_+-\varepsilon_-=\sqrt{\left(\frac{\mu}{2}\left(1+\frac{\eta_a}{\eta_{b,\mathrm{eq}}}\right)\right)^2+\frac{\eta_a\mu}{\eta_{b,\mathrm{eq}}}-\eta_a^2(1+\mu)}. \tag{29}$$

For the limiting case of low damping, $\eta_a \to 0$, this reduces to $\mu/2$, in agreement with Eq. (12). When η_a is not small and $\mu \ll 1$, the bandwidth in Eq. (29) can be approximated by

$$\frac{\delta\omega}{\omega_a}\approx\sqrt{\frac{\eta_a\mu}{\eta_{b,\mathrm{eq}}}-\eta_a^2}. \tag{30}$$

Fig. 6 shows the actual bandwidth obtained for $\mu = 0.2$ at various levels of damping, determined numerically from results such as those in Fig. 5. Each plot shows the bandwidth at a particular value of equivalent loss factor. Also shown are the estimates obtained from Eq. (29). These can be seen to agree very well with the observed bandwidths in most cases. Fig. 7 shows corresponding results for $\mu = 0.5$. Agreement is found to be slightly less good for this case, as the approximations made are no longer valid when ε is not small. Also shown in Figs. 6 and 7 are the estimates obtained using the approximate expressions according to Eqs (12) and (30). It can be seen that these give good agreement at low and high values of η_a, respectively.

The bandwidth according to Eq. (30) is dominated by the first term except for very high values of η_a where the peak of the decay rate curve is approached. From Eq. (24) it will be recalled that for high damping the peak is characterised by $\eta_{b,\mathrm{eq}} = \mu/\eta_a$, which gives $\delta\omega = 0$ in Eq. (30). However, for most of the range of values considered and where $\eta_a > 0.01$, a reasonable estimate is given by

$$\frac{\delta\omega}{\omega_a}\approx\sqrt{\frac{\eta_a\mu}{\eta_{b,\mathrm{eq}}}}. \tag{31}$$

This shows directly the benefit of increasing the absorber damping and mass ratio on the bandwidth, provided that the absorber loss factor is not increased too far.

It may be noted from these results that the relative bandwidth of the absorber is independent of the beam wavenumber, see Eq. (29). Thus by selecting an appropriate tuning frequency, such an absorber can be used to treat any frequency. In particular, it can be effective even at low frequencies where the wavelength in the beam is too long for constrained layer damping treatments to be used successfully.

6. Multiple tuning frequencies

It is worthwhile considering the potential benefit of dividing the absorber mass between two or more added systems tuned to different frequencies such that their bandwidths do not overlap (but are adjacent to each other). Such an approach has been used for discrete vibration neutralisers [28,29].

For a continuous system, the combined bandwidth of two such absorbers is

$$\delta\omega\approx\omega_{a,1}\sqrt{\frac{\mu_1\eta_{a,1}}{\eta_{b,\mathrm{eq}}}}+\omega_{a,2}\sqrt{\frac{\mu_2\eta_{a,2}}{\eta_{b,\mathrm{eq}}}}. \tag{32}$$

Assuming that the mass is equally divided, $\mu_1 = \mu_2 = \mu/2$, and that the loss factors are identical

$$\delta\omega\approx\left(\frac{\omega_{a,1}+\omega_{a,2}}{\sqrt{2}}\right)\sqrt{\frac{\mu\eta_a}{\eta_{b,\mathrm{eq}}}}. \tag{33}$$

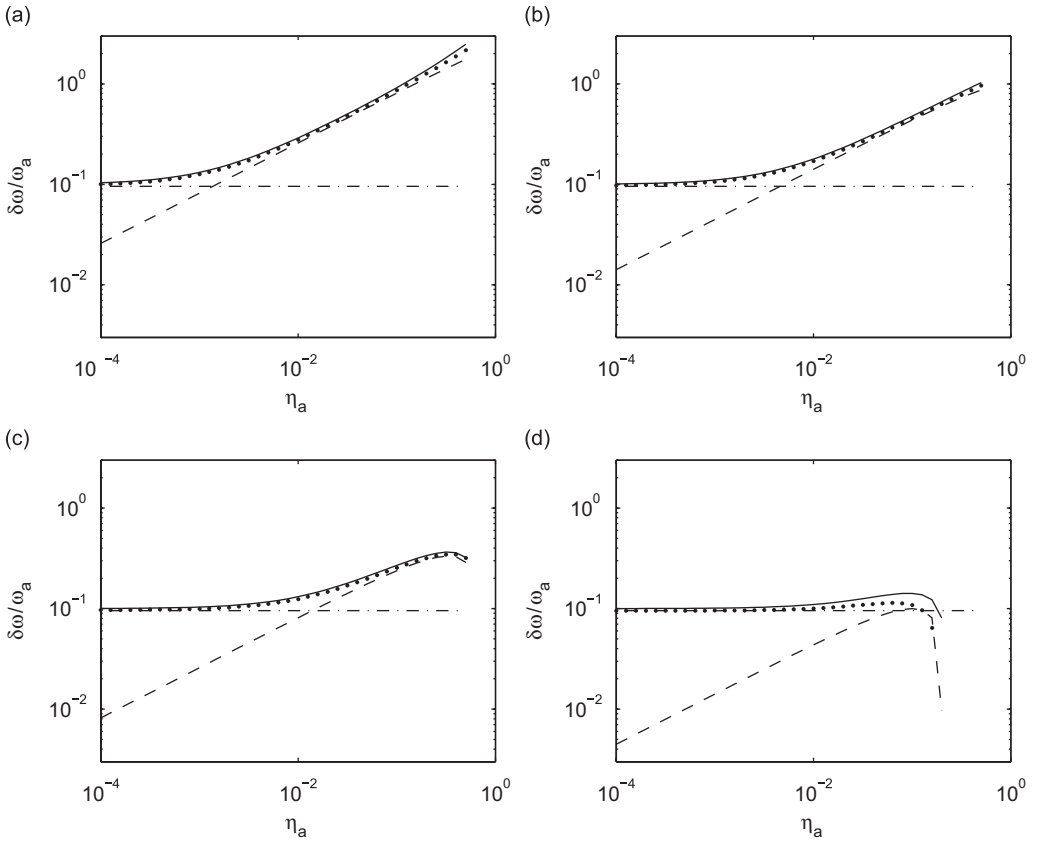

Fig. 6. Relative frequency bandwidth at various levels of equivalent loss factor, $\mu = 0.2$. (a) $\eta_{b,\mathrm{eq}} = 0.03$, (b) $\eta_{b,\mathrm{eq}} = 0.1$, (c) $\eta_{b,\mathrm{eq}} = 0.3$, (d) $\eta_{b,\mathrm{eq}} = 1$. •••••, from decay rate curves; —, full estimate, Eq. (29); – – –, simplified estimate from Eq. (30); – · – · –, estimate from undamped system, Eq. (12).

This gives a bandwidth that is wider than for a single absorber of the same overall mass by a factor of approximately $\sqrt{2}$ provided that the first term in Eq. (30) remains dominant. Similarly, dividing the mass equally between three absorbers of different frequencies leads to a bandwidth which is $\sqrt{3}$ wider than the single absorber, etc. However, as the mass is divided further, the height of each damping peak is reduced so that it becomes more difficult to obtain high decay rates. Thus there is a trade-off between bandwidth and high decay rate.

Fig. 8 shows results calculated for single, double and triple absorbers with a loss factor of 0.4 and the same combined mass of $\mu = 0.2$. Also shown is a result for ten absorbers with the same combined mass. The tuning frequencies have been chosen in each case to ensure that the equivalent loss factor $\eta_{b,\mathrm{eq}}$ just remains above 0.1 in a continuous frequency band. Although the bandwidth is clearly increased, it can be seen that the height of the peaks is reduced. The net effect for a broad-band excitation can be found by integrating the curves in Fig. 8 over frequency and is only the equivalent of 1.2 dB greater for ten absorbers than for one, although the actual benefit in practice will depend on the form of the excitation spectrum. The result for ten absorbers can be seen to be close to a limiting case such that, if the mass is further subdivided while maintaining the same beam loss factor, no further gain is obtained.

The peaks can be observed to increase slightly in height with increasing frequency, due to the influence of $k_b \propto \omega^{1/2}$. This suggests that if the target is for a particular value of decay rate, it would be more efficient to divide the mass unevenly between the various tuning frequencies, with more mass concentrated at the lower tuning frequencies.

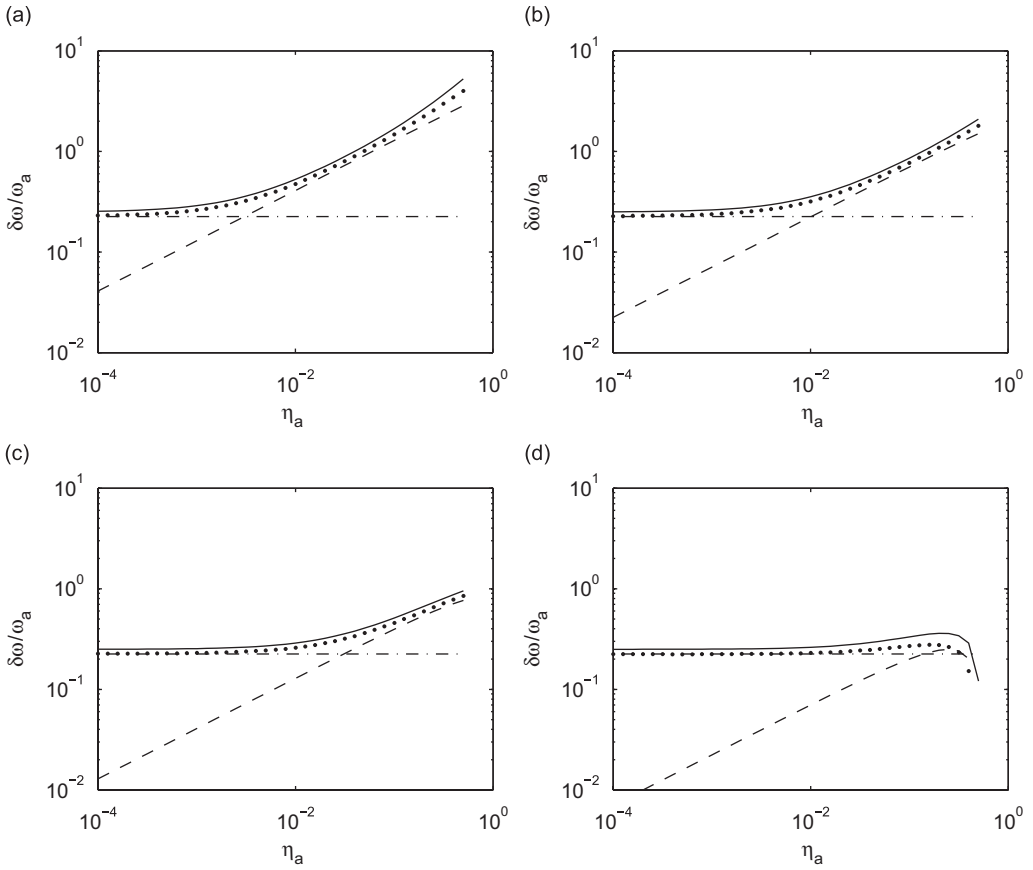

Fig. 7. Relative frequency bandwidth at various levels of equivalent loss factor, $\mu = 0.5$. (a) $\eta_{b,\mathrm{eq}} = 0.03$, (b) $\eta_{b,\mathrm{eq}} = 0.1$, (c) $\eta_{b,\mathrm{eq}} = 0.3$, (d) $\eta_{b,\mathrm{eq}} = 1$. •••••, from decay rate curves; —, full estimate, Eq. (29); – – –, simplified estimate from Eq. (30); – · – · –, estimate from undamped system, Eq. (12).

7. Absorber applied to beam on elastic foundation

If an absorber system is applied to a beam on an elastic foundation, the dynamic behaviour should be predicted by combining the foundation stiffness and the equivalent stiffness of the absorber in Eq. (7) to give a total frequency-dependent stiffness $s(\omega)$. However, since the absorber is designed to increase the attenuation of propagating waves in the region above the cut-off frequency due to the support, it is reasonable to assume that $\omega_0 \ll \omega_a$. Where these frequencies are well separated, it is possible to predict the vibration decay rate as the sum of that of the supported beam with no absorber and of the free beam with absorber. Such an approach has been used previously in determining the decay rates of a rail absorber [5], in order to simplify the analysis. In this section, the validity of this approach is investigated.

Including the foundation stiffness s_1 into Eq. (7), gives (in the absence of damping)

$$s(\omega) = s_1 + \frac{\omega^2 s_a}{\omega^2 - \omega_a^2}. \tag{34}$$

This yields a cut-off frequency, satisfying $m_r'\omega^2 - s(\omega) = 0$, which for $\omega \ll \omega_a$ gives

$$\omega'_0 \approx \sqrt{\frac{s_1}{m'_b + m'_a}} = \frac{\omega_0}{\sqrt{1+\mu}}. \tag{35}$$

This is lower than that in the absence of the absorber, due to the addition of the absorber mass. Waves are blocked below ω_0'.

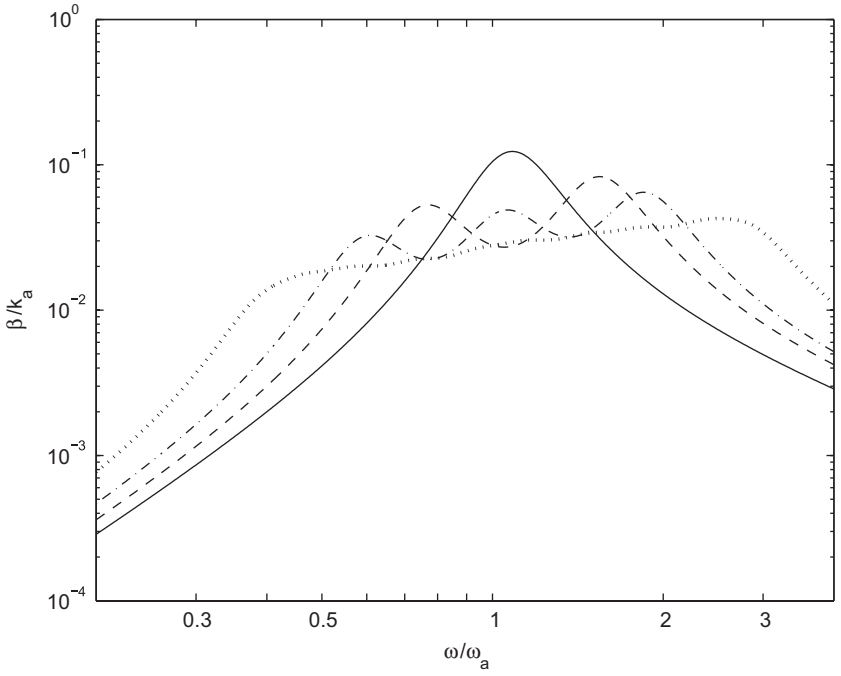

Fig. 8. Decay rate of beam with tuned absorbers, $\eta_a = 0.4$. —, single absorber with $\mu = 0.2$ tuned to ω_a; – – –, two absorbers each with $\mu_i = 0.1$ tuned to $0.72\omega_a$ and $1.45\omega_a$; – · – · –, three absorbers each with $\mu_i = 0.067$, tuned to $0.57\omega_a$, ω_a and $1.75\omega_a$; · · · · · ·, ten absorbers each with $\mu_i = 0.02$, tuned to frequencies between $0.38\omega_a$ and $2.7\omega_a$.

Including damping in each of the springs and the beam itself, the imaginary part of the wavenumber is given by a modified form of Eq. (15),

$$\beta = -\mathrm{Im}\left\{k_b(1+\mathrm{i}\eta_b)^{-1/4}\left(1-\frac{\omega_0^2}{\omega^2}(1+\mathrm{i}\eta)-\frac{\mu(1+\mathrm{i}\eta_a)}{(\omega^2/\omega_a^2)-(1+\mathrm{i}\eta_a)}\right)^{1/4}\right\}. \tag{36}$$

Around and above ω_a the final term, related to the absorber, dominates and the decay rate can be estimated using the relations in Section 4. For $\omega \gg \omega_a$,

$$\beta \approx k_b\left(\frac{\eta_b}{4}+\frac{\eta\omega_0^2}{4\omega^2}+\frac{\eta_a\mu\omega_a^2}{4\omega^2}\right). \tag{37}$$

The first two terms represent the damping effect of the beam and foundation layer, respectively, given by Eq. (6) and the third term is that of absorber above its tuning frequency, Eq. (16). This shows that the damping effects can be simply combined by adding the separate decay rates.

For frequencies well below ω_a, Eq. (36) may be expressed as

$$\beta \approx -k_b(1+\mu)^{1/4}\mathrm{Im}\left\{(1+\mathrm{i}\eta_b)^{-1/4}\left(1-\frac{\omega_0^2}{\omega^2}\frac{(1+\mathrm{i}\eta)}{(1+\mu)}\right)^{1/4}\right\}, \tag{38}$$

which is equivalent to the result in Eq. (6) for a beam of mass $m_b'(1+\mu)$ on the elastic foundation. Thus the absorber actually reduces the attenuation in this region, due to the increase in mass and the corresponding shift in cut-off frequency ω_0'.

Fig. 9 shows the normalised decay rate in the form of β/k_a for the beam on elastic foundation with absorber, according to Eq. (36). In Fig. 9(a) the initial cut-off frequency for the beam on elastic foundation ω_0 is set to $0.3\omega_a$ and $\mu = 0.2$. For simplicity the beam damping loss factor η is set to zero. In addition, the separate results are shown for the beam on elastic foundation and the unsupported beam with absorber. As noted above, the effective cut-off frequency due to the support stiffness is reduced, here by about 9%, and

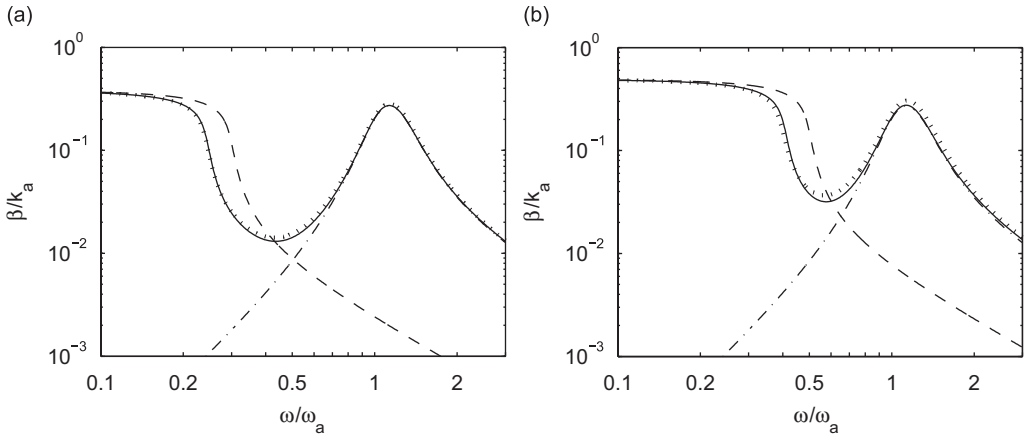

Fig. 9. Normalised decay rate of supported beam with tuned absorbers, $\mu = 0.2$, $\eta = 0.1$, $\eta_a = 0.4$, (a) $\omega_0 = 0.3\omega_a$, (b) $\omega_0 = 0.5\omega_a$. · · · · · ·, direct calculation of supported beam with absorber; – · – · , absorber on free beam; – – –, supported beam with no absorber; —, sum of decay rates of absorber on free beam and supported beam including absorber mass.

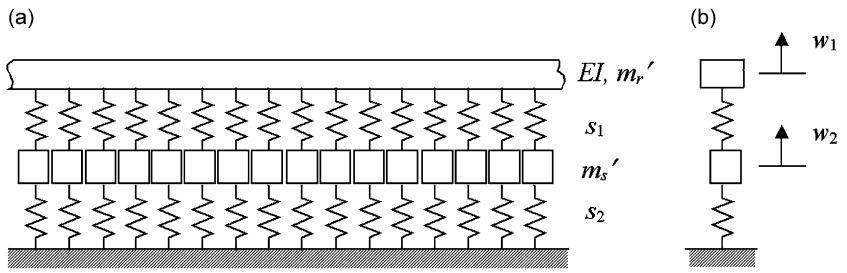

Fig. 10. (a) Beam on two-layer foundation, (b) equivalent mass–spring system.

consequently the decay rate is reduced slightly in the region between about $0.2\omega_a$ and $0.5\omega_a$ (around and above ω_0) by the addition of the absorber mass. By adjusting the mass of the beam to include that of the absorber, a good approximation to the exact result can be obtained using the sum of the two separate results.

In Fig. 9(b) results are shown for a stiffer support, giving $\omega_0 = 0.5\omega_a$, again with $\mu = 0.2$. Here, in the vicinity of ω_a, the combined effect is slightly larger than predicted by adding the separate effects. However, the difference is still less than 1 dB and the approximate approach is acceptable.

8. Two-layer foundation

In this section a beam on a two-layer foundation is considered, as shown in Fig. 10. This can represent, for example, a railway track consisting of a rail supported on sleepers, with resilient rail pads between the rail and sleeper and ballast beneath the sleeper providing a further layer of resilience. It has long been recognised that the sleeper mass forms a dynamic absorber which increases the rail decay rate in a particular frequency band [30]. The effect of including the absorber mass within the foundation in this way is investigated here. The stiffness per unit length of the upper spring is denoted s_1, the mass per unit length of the intermediate mass is m_s' and s_2 is the stiffness per unit length of the lower spring.

The analysis of Section 3 can be repeated but with a frequency-dependent support stiffness, $s(\omega)$, which in the undamped case is given by

$$s(\omega) = \frac{s_1(s_2 - \omega^2 m'_s)}{(s_1 + s_2 - \omega^2 m'_s)}. \tag{39}$$

Damping can be added as before by making s_1 and s_2 complex with loss factors η_1 and η_2, respectively. If the beam is constrained, the mass m_s' can vibrate freely on the combined stiffness of the two layers at the frequency ω_a, given by

$$\omega_a = \sqrt{\frac{s_1 + s_2}{m'_s}}. \tag{40}$$

This corresponds to an *anti*-resonance of the support as seen at the beam and is the tuning frequency of the two-layer support at which it acts as a neutraliser to the beam.

There are two frequencies at which $m_r'\omega^2 - s(\omega) = 0$, corresponding to the condition of cut-off seen in Section 3. These are the natural frequencies of the corresponding two-degree-of-freedom system shown in Fig. 10(b). They can be found as

$$\omega_c^2 = \frac{(\omega_1^2 + \omega_a^2)}{2} \pm \sqrt{\frac{(\omega_1^2 + \omega_a^2)^2}{4} - \omega_1^2\omega_2^2}, \tag{41a}$$

where ω_1 and ω_2 are given by

$$\omega_1 = \sqrt{\frac{s_1}{m'_r}}, \quad \omega_2 = \sqrt{\frac{s_2}{m'_s}}. \tag{41b,c}$$

The two cut-off frequencies ω_c are plotted in Fig. 11 for different values of $\mu = m'_s/m'_b$ and $\kappa = s_1/s_2$. These results have been normalised by the absorber tuning frequency ω_a from Eq. (40). The absorber bandwidth $[\omega_a, \omega_{c2}]$ can be seen to be smaller than the corresponding result from Eq. (12), shown by the circles, which forms the limit as $s_2 \to 0$.

Examples of the wavenumbers are shown in Fig. 12, normalised to the free beam wavenumber at ω_a. These results are given for $\mu = 4$, which is typical of a railway track with concrete sleepers [30], although much larger than considered in earlier sections.

As for the case of a single stiffness support, below the first cut-off frequency ω_{c1}, a low frequency 'blocked' region occurs where no waves propagate, the wavenumbers having equal real and imaginary parts. Free wave

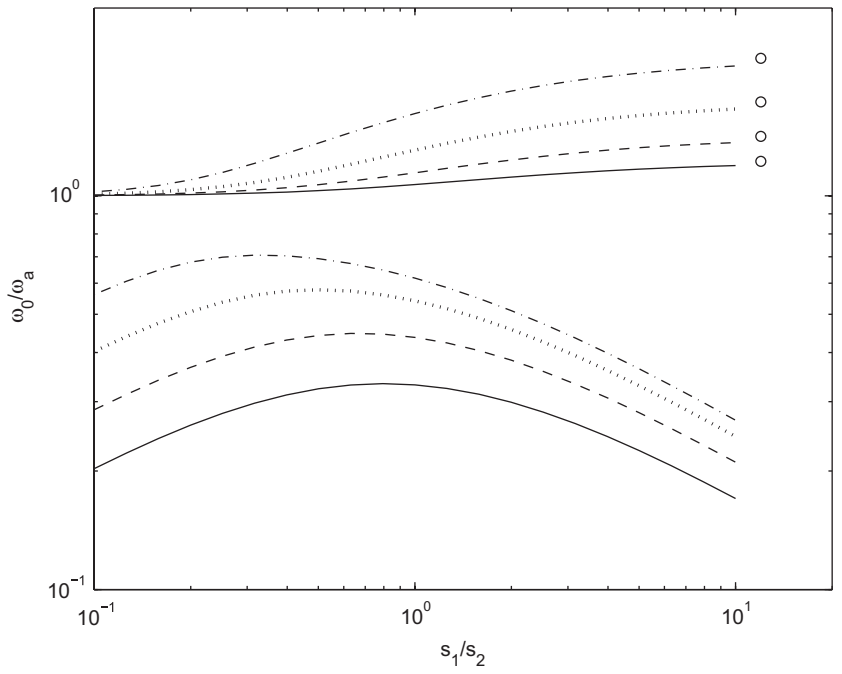

Fig. 11. Bounding frequencies of propagating wave behaviour shown relative to 'absorber tuning frequency' of two-layer foundation. —, $\mu = 0.5$; – – –, $\mu = 1$; · · · · · ·, $\mu = 2$; – · – · –, $\mu = 4$; o, limit for $s_2 = 0$.

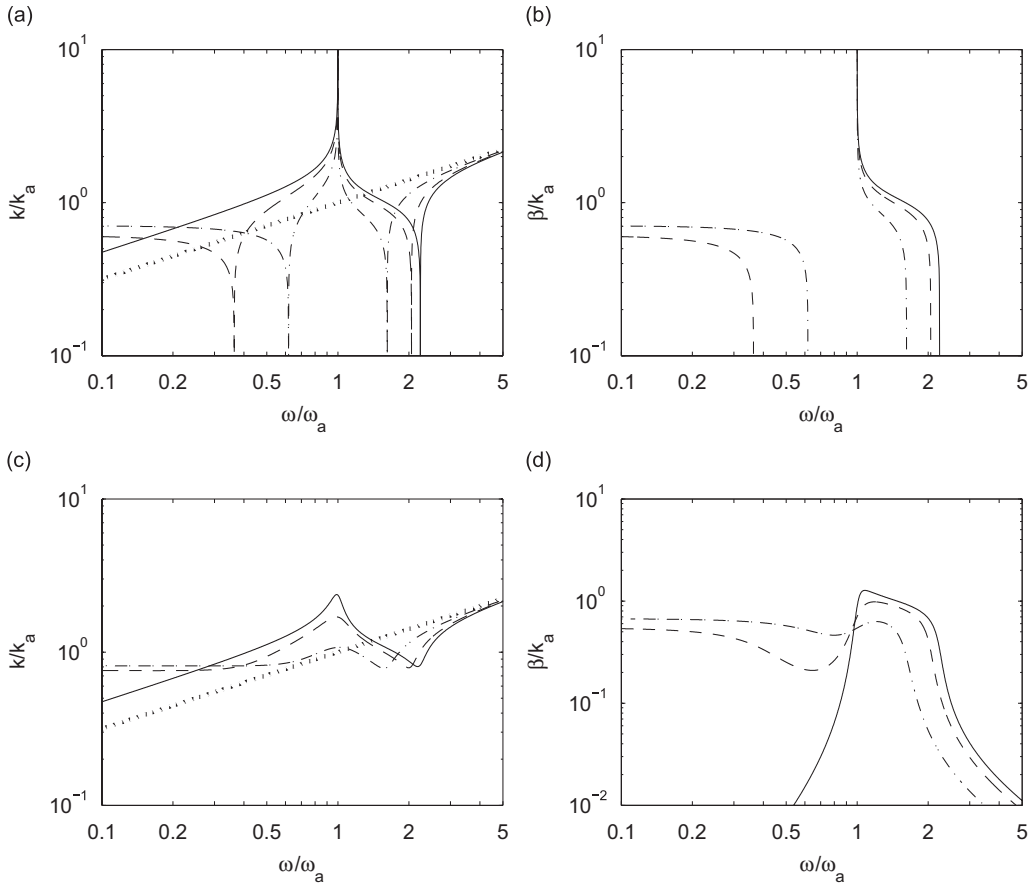

Fig. 12. First wavenumber for beam on two-layer foundation, $\mu = 4$. —, $\kappa = \infty$ ($s_2 = 0$); – – –, $\kappa = 5$; – · – · $\kappa = 1$, · · · · · ·, free beam. Frequency normalised by ω_a, wavenumbers by beam free wavenumber at ω_a. (a) Real part of first wave, undamped, (b) imaginary part of first wave, undamped, (c) real part of first wave, $\eta_1 = 0.1$, $\eta_2 = 1$, and (d) imaginary part of first wave, $\eta_1 = 0.1$, $\eta_2 = 1$.

propagation occurs in the whole of the region between ω_{c1} and ω_a. At ω_a the support stiffness $s(\omega)$ becomes infinite and changes sign and free wave propagation ceases. There follows a second 'blocked' region of complex wavenumbers between ω_a and ω_{c2}, in which the wavenumber falls with increasing frequency, above which free wave propagation again commences. At high frequency the wavenumber tends to that of the unsupported beam, k_b. The region between ω_a and ω_{c2} resembles closely that of the absorber seen in Section 4.

As the stiffness of the lower layer (s_2) increases, relative to s_1, the width of the blocked zone above ω_a reduces, making the absorber less effective. Conversely, the blocked region at low frequency extends higher in frequency.

Also shown in Fig. 12 are results including damping in the support layers. These show similar trends to the undamped results, with the 'blocked' regions still discernible below ω_{c1} and between ω_a and ω_{c2}. The attenuation (imaginary part) is no longer zero outside these blocked regions. As for the undamped case, the effectiveness of the intermediate mass acting as an absorber can be seen to reduce as the stiffness of the lower layer increases. For smaller values of μ, not shown, the bandwidth of the absorber peak is reduced.

This confirms that the sleeper in a railway track acts like a tuned absorber. Since it has quite large mass compared with the beam, large attenuation is possible over a wide frequency range. The effectiveness is reduced, however, as the stiffness of the upper resilient layer is reduced relative to that of the lower layer.

9. Conclusions

The use of a continuous, damped mass–spring system added to a beam has been shown to be effective in increasing the attenuation of propagating structural waves in the beam and hence reducing the radiated noise. It is effective at any tuning frequency, independent of the bending wavelength in the beam, and so is particularly useful for stiff beams or at low frequencies, where constrained layer damping would be impractical. This has been developed for the particular application to a railway track [5] but could also be considered for piping systems and many other beam-like structures. The practical application considered in [5] consists of steel masses embedded in an elastomer attached to the rail. Multiple tuning frequencies and a high damping loss factor are used to give attenuation over a broad frequency range.

Approximate formulae for the effect have been derived. The effective frequency bandwidth increases as the mass ratio of the absorber to the beam is increased. Although the bandwidth is independent of the absorber damping loss factor for low damping, for moderate-to-high damping the bandwidth increases as the damping is increased. The maximum decay rate is independent of mass and damping for light damping, but for higher damping it reduces as loss factor increases and increases as the mass ratio increases. For a given mass, the effective bandwidth can also be increased by dividing the mass to form multiple absorbers with different tuning frequencies, although the height of the decay rate peak is reduced as a result.

For a beam on an elastic foundation, the addition of an absorber can be represented well by adding the decay rates of the unsupported beam with absorber and the supported beam without absorber but including the absorber mass.

For a railway track with concrete sleepers, the mass of the sleeper acts as a tuned absorber which increases the decay rate over a wide frequency region. The large mass relative to the rail makes this an effective system. However, the fact that the absorber is integral to the support system in this case means that the benefit is less than that for a separate absorber of the same mass, especially if the rail pad is not much stiffer than the ballast layer below the sleeper.

Acknowledgements

The analysis described here was carried out partly during a period of sabbatical leave in September 2005. The author is grateful to Trinity College, Cambridge for providing a Visiting Scholarship, to the Engineering Department of the University of Cambridge which hosted him during this period and to Dr. Hugh Hunt in particular.

References

[1] K.F. Graff, *Wave Motion in Elastic Solids*, Dover Publications, New York, 1991.
[2] L. Cremer, M. Heckl, E.E. Ungar, *Structure-borne Sound*, second ed., Springer, Berlin, 1988.
[3] D.J. Thompson, C.J.C. Jones, N. Turner, Investigation into the validity of two-dimensional models for sound radiation from waves in rails, *Journal of the Acoustical Society of America* 113 (2003) 1965–1974.
[4] C.J.C. Jones, D.J. Thompson, R.J. Diehl, The use of decay rates to analyse the performance of railway track in rolling noise generation, *Journal of Sound and Vibration* 293 (2006) 485–495.
[5] D.J. Thompson, C.J.C. Jones, T.P. Waters, D. Farrington, A tuned damping device for reducing noise from railway track, *Applied Acoustics* 68 (2007) 43–57.
[6] D.J. Thompson, P.-E. Gautier, A review of research into wheel/rail rolling noise reduction, *Proceedings of the Institution of Mechanical Engineers, Part F* 220F (2006) 385–408.
[7] D.J. Mead, *Passive Vibration Control*, Wiley, Chichester, 2000.
[8] V.V. Krylov, New type of vibration dampers utilising the effect of acoustic 'black holes', *Acta Acustica United with Acustica* 90 (2004) 830–837.
[9] A.D. Nashif, D.I.G. Jones, J.P. Henderson, *Vibration Damping*, Wiley, New York, 1985.
[10] J.A. Zapfe, G.A. Lesieutre, Broadband vibration damping using highly distributed tuned mass absorbers, *AIAA Journal* 35 (1997) 753–755.
[11] M.J. Brennan, N.S. Ferguson, Vibration control, in: F. Fahy, J. Walker (Eds.), *Advanced Applications of Acoustics, Noise and Vibration*, E&FN Spon, London, 2004 (Chapter 12).
[12] J.B. Hunt, *Dynamic Vibration Absorbers*, Mechanical Engineering Publications, London, 1979.

[13] M.J. Brennan, Vibration control using a tunable vibration neutralizer, *Proceedings of the Institution of Mechanical Engineers, Part C* 211C (1997) 91–108.
[14] J. Ormondroyd, J.P. Den Hartog, The theory of the dynamic vibration absorber, *Transactions of the American Society of Mechanical Engineers* 50 (1928) A9–A22.
[15] J.P. Den Hartog, *Mechanical Vibrations*, Dover Publications, New York, 1985.
[16] R. Rana, T.T. Soong, Parametric study and simplified design of tuned mass dampers, *Engineering Structures* 20 (1998) 193–204.
[17] D.E. Newland, Vibration of the London Millennium Bridge: cause and cure, *International Journal of Acoustics and Vibration* 8 (2003) 9–14.
[18] D.E. Newland, Pedestrian excitation of bridges, *Proceedings of the Institution of Mechanical Engineers, Part C* 218C (2004) 477–492.
[19] S. Zivanovic, A. Pavic, P. Reynolds, Vibration serviceability of footbridges under human-induced excitation: a literature review, *Journal of Sound and Vibration* 279 (2005) 1–74.
[20] P. Clark, Devices for the Reduction of Pipeline Vibration, PhD thesis, University of Southampton, 1995.
[21] M.J. Brennan, Control of flexural waves on a beam using a tunable vibration neutraliser, *Journal of Sound and Vibration* 222 (1998) 389–407.
[22] V.I. Kashina, V.V. Tyutekin, Waveguide vibration reduction of longitudinal and flexural modes by means of a multielement structure of resonators, *Soviet Physics Acoustics* 36 (1990) 383–385.
[23] T.L. Smith, K. Rao, I. Dyer, Attenuation of plate flexural waves by a layer of dynamic absorbers, *Noise Control Engineering Journal* 26 (1986) 56–60.
[24] M. Strasberg, D. Feit, Vibration damping of large structures induced by attached small resonant structures, *Journal of the Acoustical Society of America* 99 (1996) 335–344.
[25] C.R. Fuller, J.P. Maillard, M. Mercadal, A.H. von Flowtow, Control of aircraft interior noise using globally detuned vibration absorbers, *Journal of Sound and Vibration* 203 (1997) 745–761.
[26] P. Marcotte, C.R. Fuller, P. Cambou, Control of the noise radiated by a plate using a distributed active vibration absorber (DAVA), *Proceedings of Active 99*, Ft Lauderdale, FL, USA, 1999, pp. 447–456.
[27] S.J. Estève, M.E. Johnson, Reduction of sound transmission into a circular cylindrical shell using distributed vibration absorbers and Helmholtz resonators, *Journal of the Acoustical Society of America* 112 (2002) 2840–2848.
[28] M.J. Brennan, Characteristics of a wideband vibration neutralizer, *Noise Control Engineering Journal* 45 (1997) 201–207.
[29] G. Maidanik, K.J. Becker, Characterization of multiple-sprung masses for wideband noise control, *Journal of the Acoustical Society of America* 106 (1999) 3109–3118.
[30] D.J. Thompson, N. Vincent, Track dynamic behaviour at high frequencies. Part 1: theoretical models and laboratory measurements, *Vehicle System Dynamics Supplement* 24 (1995) 86–99.